

# Tungsten(6+) Tris(pinacolate): Structure and Comments on the Preference for an Octahedral Geometry Relative to Trigonal Prismatic ( $D_{3h}$ ) for a $d^0$ Complex in the Presence of Strong $\pi$ -Donor Ligands

M. H. Chisholm,\* Ivan P. Parkin, William E. Streib, and O. Eisenstein\*

Department of Chemistry and Molecular Structure Center, Indiana University, Bloomington, Indiana 47405, and Laboratoire de Chimie Théorique, Bâtiment 490, Université de Paris-Sud, 91405 Orsay, France

Received September 29, 1993\*

The reaction between  $W(NMe_2)_6$  and  $HOCMe_2CMe_2OH$  (pinacol, 3 equiv) in ether/hexanes yields the pale yellow compound  $W(OCMe_2CMe_2O)_3$  (**1**) as pale yellow cubic crystals. Crystal data at  $-155\text{ }^\circ\text{C}$ :  $a = 16.841(2)\text{ \AA}$ ,  $b = 9.878(1)\text{ \AA}$ ,  $c = 13.373(1)\text{ \AA}$ ,  $\beta = 109.60(1)^\circ$ ,  $Z = 4$ ,  $d_{\text{calcd}} = 1.69\text{ g cm}^{-3}$ , space group  $C2/c$ . The molecule has a crystallographically imposed  $C_2$  axis of symmetry but may basically be described as having a distorted octahedral  $WO_6$  core,  $W-O = 1.92(1)\text{ \AA}$  (average). Variable-temperature  $^1H$  NMR data reveal two Me proton signals ( $+80$  to  $-80\text{ }^\circ\text{C}$ ) in toluene- $d_8$  and thus indicate that enantiomerization via a trigonal prismatic intermediate is slow on the NMR time scale. The preference for the  $d^0$ -octahedral  $WO_6$  geometry is explained on the basis of oxygen  $p_\pi$  to  $W d_\pi$  bonding, and these results are compared with those for other  $d^0$ - $ML_6$  complexes and  $d^0$ - $M(\text{chelating ligand})_3$  complexes.

## Introduction

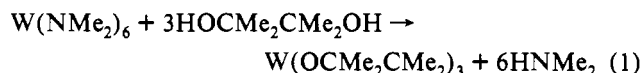
Most of the hexacoordinated transition metal complexes are octahedral. This is in particular the case of  $d^6$  complexes where angular distortion away from ideal  $90^\circ$  angles are due to the steric demands of the coordinated ligands. Lower electron counts at the metal result in a higher variety of structures: octahedral, trigonal prismatic notably in the case of  $d^0$  metal centers,<sup>1–8</sup> and bicapped tetrahedra in the case of  $d^4$  metal centers.<sup>1,9–11</sup> The  $d^0$  systems have been especially controversial. VSEPR rules would give a preference for an octahedral geometry. The original proposal,<sup>1,2</sup> based on a second-order Jahn–Teller argument that  $d^0$ - $MR_6$  ( $R = \text{pure } \sigma\text{-donor ligands}$ ) may not have an octahedral geometry has been challenged by state of the art ab initio calculations,<sup>3</sup> and contradictory results have been obtained. A consensus has been reached on  $d^0$ - $MH_6$ . The equilibrium geometry has been calculated to be of either  $D_{3h}$  or  $C_{3v}$  symmetry for different metal centers.<sup>4,5</sup> Experimental data have supported these theoretical results since  $WMe_6$  has been found to have  $D_{3h}$  symmetry by electron diffraction.<sup>8a</sup> Recent theoretical studies have confirmed that  $MH_6$  and  $MMe_6$  have similar structural properties.<sup>8b</sup> Replacing pure  $\sigma$ -donor ligands by  $\pi$ -donor ligands decreases the tendency for distortion away from  $O_h$  symmetry since it increases the HOMO–LUMO gap. Contradictory results have appeared in the case of  $CrF_6$  probably because F is a moderate

$\pi$  donor.<sup>4,5</sup> It is probable that the potential energy surface describing the structural distortion away from  $O_h$  symmetry is rather flat for such species. Experimental data on the elusive  $CrF_6$  complex are in support of an octahedral structure, but this matter continues to be discussed extensively in the literature.<sup>12–14</sup> Better  $\pi$  donors than F should certainly increase the preference for  $O_h$  symmetry.

We report here the synthesis and characterization of tungsten(6+) tris(pinacolate),  $W(OCMe_2CMe_2O)_3$  (**1**), and show that, despite the presence of the three chelating ligands, the barrier to enantiomerization via a trigonal prismatic  $D_{3h}$  geometry is slow on the NMR time scale. The preference for octahedral geometry, albeit distorted, is understood in terms of oxygen  $p_\pi$  to tungsten  $d_\pi$  bonding.

## Results and Discussion

**Synthesis.** The reaction between 3 equiv of pinacol and tungsten hexakis(dimethylamide) in diethyl ether/hexane produces tungsten tris(pinacolate) in high yield (eq 1). Monitoring the reaction



by  $^1H$  NMR spectroscopy showed the production of  $HNMe_2$  but revealed no detectable tungsten-containing intermediates. The substitution reactions of  $W(NMe_2)_6$  with alcohols have been studied, and complexes of formulas  $W(OMe)_6$  and  $W(OEt)_6$  have been synthesized.<sup>15</sup> For larger alcohols such as *t*-BuOH and neopentanol, no reaction with  $W(NMe_2)_6$  occurs at room temperature. Presumably, steric hindrance prevents alcoholysis. Thus it is noteworthy that pinacol, which has essentially the same steric shielding at the  $\alpha$ -carbon as *t*-BuOH, undergoes substitution reactions with  $W(NMe_2)_6$ . The  $pK_a$  of pinacol is smaller (more

\* To whom correspondence should be addressed: M.H.C., Indiana University; O.E., Université de Paris-Sud.

† Abstract published in *Advance ACS Abstracts*, January 15, 1994.

- (1) Hoffmann, R.; Howell, J. M.; Rossi, A. R. *J. Am. Chem. Soc.* **1976**, *98*, 2484.
- (2) Demolliens, A.; Jean, Y.; Eisenstein, O. *Organometallics* **1986**, *5*, 1457.
- (3) Cameron, A. D.; Fitzgerald, G.; Zerner, M. C. *Inorg. Chem.* **1988**, *27*, 3437.
- (4) Kang, S. K.; Albright, T. A.; Eisenstein, O. *Inorg. Chem.* **1989**, *28*, 1611.
- (5) Marsden, C. J.; Wolyne, P. P. *Inorg. Chem.* **1991**, *30*, 1681.
- (6) Jonas, V.; Frenking, G.; Gauss, J. *Chem. Phys. Lett.* **1992**, *194*, 109.
- (7) Hope, E. G.; Levason, W.; Ogden, J. S. *Inorg. Chem.* **1991**, *30*, 4874.
- (8) (a) Haaland, A.; Hammel, A.; Rypdal, K.; Volden, H. V. *J. Am. Chem. Soc.* **1990**, *112*, 4547. (b) Kang, S. K.; Tang, H.; Albright, T. A. *J. Am. Chem. Soc.* **1993**, *115*, 1971.
- (9) Kubacek, P.; Hoffmann, R. *J. Am. Chem. Soc.* **1981**, *103*, 4320.
- (10) Templeton, J. L.; Winston, P. B.; Ward, B. C. *J. Am. Chem. Soc.* **1981**, *103*, 7713.
- (11) Kamata, M.; Hirotsu, K.; Higuchi, T.; Tatsumi, K.; Hoffmann, R.; Yoshida, T.; Otsuka, S. *J. Am. Chem. Soc.* **1981**, *103*, 5772.

(12) Pierlott, K.; Roos, B. O. *Inorg. Chem.* **1992**, *31*, 5353.

(13) Neuhaus, A.; Frenking, G.; Huber, C.; Gauss, J. *Inorg. Chem.* **1992**, *31*, 5355.

(14) Jacobs, J.; Müller, H. S. P.; Willner, H.; Jacob, E.; Bürger, H. *Inorg. Chem.* **1992**, *31*, 5357.

(15) Chisholm, M. H.; Extine, M. W.; Stager, M. W. *Inorg. Chem.* **1977**, *16*, 1794.

acidic) than that of *t*-BuOH,<sup>16</sup> and probably the chelate effect of the diolate ligand makes subsequent coordination more accessible.

**Characterization.** Tungsten tris(pinacolate) was characterized by VT <sup>1</sup>H NMR, IR, melting point, mass spectrometry, microanalysis, and X-ray crystallography. The compound crystallizes as pale yellow cubes by cooling of a saturated diethyl ether/hexane solution. It is air stable both in solution and in the solid state (for over a year), soluble in aromatic and aliphatic hydrocarbon solvents, and unreactive toward alcoholysis by MeOH and EtOH. On heating to 182 °C, it decomposes. However, an electron impact mass spectrum did detect the parent ion at 534 amu with the correct isotopic abundances for an included tungsten atom. Other fragmentation peaks occur at  $M^+ - C(CH_3)_2H$ ,  $M^+ - OC(CH_3)_2H$ , and  $M^+ - C_2Me_4O_2$ , all with the correct tungsten isotopic correlations.

The IR spectrum of  $W(O_2C_2Me_4)_3$  shows the expected pinacolate vibrations.

**Solution-State <sup>1</sup>H NMR.** The <sup>1</sup>H NMR of  $W(O_2C_2Me_4)_3$  is temperature invariant in  $C_6D_5CD_3$  from -90 to +110 °C and shows two resonances of equal intensity at  $\delta = 1.54, 1.12$  ppm. This implies that there are two different environments for the methyl groups in  $W(O_2C_2Me_4)_3$ . The solid-state structure of  $W(O_2C_2Me_4)_3$  shows one  $C_2$  axis and one pseudo- $C_3$  axis. In solution the five-membered rings will be expected to be undergoing rapid ring flipping even at -90 °C on the NMR time scale. The rapid interconversion of the  $C_2$  axis by ring flipping generates on the NMR time scale effectively three  $C_2$  axes, and this makes all three rings equivalent. However, this process does not make the four methyl groups on each pinacolate ligand equivalent. For each  $M(\text{chelating ligand})_3$  enantiomer, with time-averaged  $D_3$  symmetry, there will be two sets of Me ligands. However, if the  $WO_6$  core were stereochemically labile with respect to enantiomerization, *i.e.* attainment of a trigonal prismatic geometry, then the combined ring flipping and  $WO_6$  skeletal rearrangements would lead to only one time-averaged Me signal. The barrier for enantiomerization involving a trigonal prismatic geometry must then be greater than 15 kcal mol<sup>-1</sup>. Of course, a fluxional process based on W-O bond cleavage might have been possible—this too is ruled out by the NMR behavior and is presumably less likely for a  $W^{6+}$ -containing compound with three dianionic chelates than, *e.g.*, for a  $M^{3+}(\text{chelating ligand})_3$  complex where the ligand has a uninegative charge, as for example in  $M(\text{acac})_3$  complexes where  $M = Al, In, Ga$  and *acac* is the anion derived from deprotonation of 2,5-pentanedione.<sup>17</sup>

**Crystal and Molecular Structure of  $W(O_2C_2Me_4)_3$  (1).** In the space group  $C2/c$  there is one unique molecule of  $W(O_2C_2Me_4)_3$  in the unit cell. Two views of the molecule are given in Figure 1, and selected bond lengths and angles are given in Table 1. A summary of the crystal data is given in Table 2. The compound has a distorted octahedral  $WO_6$  moiety and a crystallographically imposed 2-fold axis of symmetry bisecting O(10), O(10)', and W(1). The structure is very similar to that adopted by  $W(O_2C_2H_4)_3$ .<sup>18</sup>

The crystal structure of  $W(O_2C_2Me_4)_3$  is consistent with  $d^0$   $W(6+)$  being surrounded by six uninegative O-R ligands. All the W-O distances are, within the  $3\sigma$  criteria, the same in  $W(O_2C_2Me_4)_3$ , at 1.916(3) Å (average). This distance is comparable to those observed in  $W_2(OR)_6$  complexes at 1.88 Å (average)<sup>19</sup> and is consistent with some  $M d_{\pi} - O p_{\pi}$  interaction.

For  $W(O_2C_2Me_4)_3$  the twist angle  $\theta$ , as calculated from the centroids viewed down the pseudo- $C_3$  axis, is 34°. This indicates

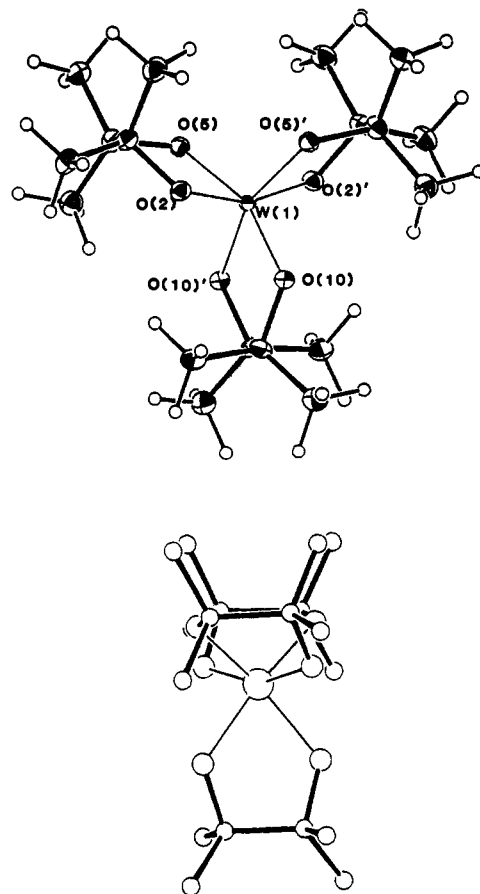


**Figure 1.** ORTEP drawing of the  $W(O_2C_2Me_4)_3$  molecule showing the atom-numbering scheme (top) and a view of the molecule viewed down the crystallographically imposed  $C_2$  axis of symmetry.

**Table 1.** Selected Bond Distances (Å) and Angles (deg) for  $W(O_2C_2Me_4)_3$  (1)

Distances			
W(1)-O(2)	1.914(3)	O(2)-C(3)	1.442(5)
W(1)-O(5)	1.915(3)	O(5)-C(4)	1.440(5)
W(1)-O(10)	1.920(3)	O(10)-C(11)	1.441(5)
Angles			
O(2)-W(1)-O(2)'	160.02(18)	O(5)-W(1)-O(10)	89.73(12)
O(2)-W(1)-O(5)	78.11(12)	O(5)-W(1)-O(10)'	158.03(12)
O(2)-W(1)-O(5)'	89.99(12)	O(5)-W(1)-O(10)'	78.15(17)
O(2)-W(1)-O(10)'	88.08(12)	W(1)-O(2)-C(3)	120.58(26)
O(2)-W(1)-O(10)	107.63(12)	W(1)-O(3)-C(4)	119.30(25)
O(5)-W(1)-O(5)'	107.08(17)	W(1)-O(10)-C(11)	119.16(25)

**Table 2.** Summary of Crystal Data for  $W(O_2C_2Me_4)_3$  (1)

empirical formula	$C_{18}H_{36}O_6W$
space group	$C2/c$
temp (°C)	-155
<i>a</i> (Å)	16.841(2)
<i>b</i> (Å)	9.878(1)
<i>c</i> (Å)	13.373(1)
$\beta$ (deg)	109.60(1)
<i>Z</i> (molecules/cell)	4
<i>V</i> (Å <sup>3</sup> )	2095.76
calcd density (g/cm <sup>3</sup> )	1.687
$\lambda$ (Å)	0.710 69
MW	532.33
$\mu$ (cm <sup>-1</sup> )	56.557
$2\theta$ range (deg)	6-45
$R(F_o \text{ or } F_c)$	0.0202
$R_w(F_o \text{ or } F_c)$	0.0218

that the molecule is very close to the common  $M(\text{bidentate})_3$  geometry of  $D_3$  ( $\theta = 30^\circ$ ) but slightly twisted toward octahedral geometry.<sup>20</sup> See Figure 2.

The oxygen atoms in  $W(O_2C_2Me_4)_3$  are almost perfectly  $sp^2$  hybridized ( $W-O-C = 120^\circ$  (average), and the O-C and C-C

(16) *pKa Prediction for Organic Acids and Bases*; Perring, D. D., Dempsey, B., Serjent, P., Eds.; Chapman and Hall: London, 1981.

(17) For a discussion of the dynamic NMR behavior of  $M(\text{chelating ligand})_3$  complexes, see: Holm, R. H. In *Dynamic NMR*; Cotton, F. A., Jackman, L. M., Eds.; Academic Press: New York, 1975; Chapter 9.

(18) Scherle, V. J.; Schröder, F. A. *Acta Crystallogr.* 1974, B20, 2772.

(19) Chisholm, M. H. *Polyhedron* 1983, 2, 681.

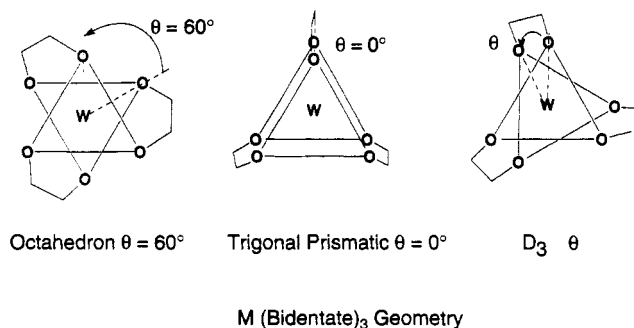


**Figure 2.** Geometries of  $M(\text{chelating ligand})_3$  complexes showing the definitions of the angle  $\theta$ .

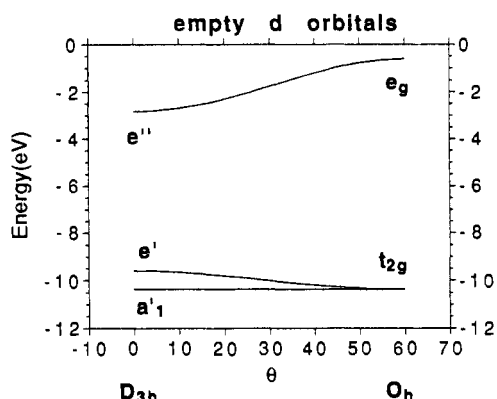


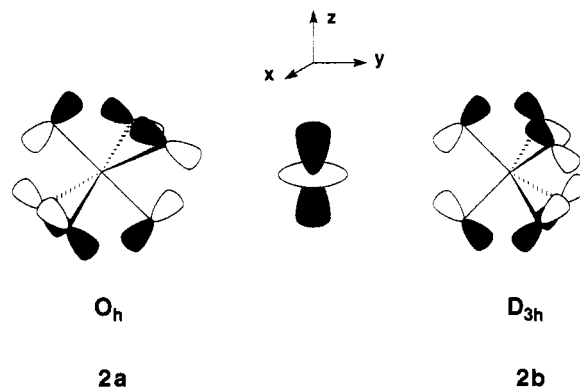
**Figure 3.** Walsh diagram of the d orbitals of  $\text{WH}_6$  in the  $O_h$  to  $D_{3h}$  transformation.

bonds, at 1.44 Å (average) and 1.53 Å (average), are normal for single (unstrained) bonds. The three five-membered rings all adopt the envelope structure. The trans O–W–O angles are all distorted away from octahedral and average 160°.

### Bonding Analysis

It has been shown that a  $d^0\text{-MX}_6$  ( $X = \text{pure } \sigma\text{-donor group}$ ) prefers to have a  $D_{3h}$  or  $C_{3v}$  structure because more metal d orbitals participate in the M–R  $\sigma$  bonds.<sup>4,8b</sup> While the X group used the metal s, p and only two of the d orbitals to make the  $\sigma$  M–X bonds in the octahedral geometry, additional metal orbitals are involved in the reduced  $D_{3h}$  or  $C_{3v}$  symmetry. This fact is evidenced in the Walsh diagram (Figure 3) which shows the behavior of the d orbitals in the  $O_h \rightarrow D_{3h}$  transformation. These orbitals, which are either nonbonding or metal–ligand antibonding, are informative of the behavior of the corresponding metal–ligand occupied orbitals. Two of the lower orbitals ( $t_{2g}$  in  $O_h$  symmetry;  $e'$  in  $D_{3h}$ ) are higher in energy in  $D_{3h}$  since they can overlap with the ligands.<sup>4,8b</sup> In the case of  $C_{3v}$  symmetry, the three “ $t_{2g}$ ” orbitals are actually used in M–X  $\sigma$  bonding. However, this increased participation in the number of d orbitals is accompanied by a diminution of the strength of the M–X interaction within the  $e_g$  set (in  $O_h$ ), as shown by the lowering energy of the “ $e_g$ ” ( $e''$  in  $D_{3h}$ ) orbitals in a  $D_{3h}$  structure. Thus, on going from  $O_h$  to  $D_{3h}$  symmetry, some occupied molecular orbitals characterizing the M–X  $\sigma$  bonds are decreasing in energy because they incorporate additional  $t_{2g}$  metal character but some are increasing because they lose some metal  $e_g$  participation. The outcome of these opposite effects, typical of a second-order Jahn–Teller (J–T) distortion, is not predictable. However, the trend is clear: in the case of low-lying  $t_{2g}$  orbitals, the increased participation of the  $t_{2g}$  orbitals dominates and the complex prefers a  $D_{3h}$  symmetry. Sophisticated calculations and experimental results have confirmed this tendency, as mentioned in the Introduction.

When X is a  $\pi$ -donor ligand, the  $t_{2g}$  metal orbitals are destabilized by  $\pi$  lone pairs of the X ligands in the  $O_h$  geometry (these interactions are responsible for the M–X multiple bonds). Therefore, according to the above argument,  $\text{MX}_6$  should have  $O_h$  geometry. Another effect reinforces this result. The  $d_{\pi}/p_{\pi}$  effects are larger in  $O_h$  geometry. This can be easily seen in particular in the case of the  $z^2$  orbital. This orbital, which is one of the  $t_{2g}$  orbitals when z is along a  $C_3$  axis, is stabilized by about 0.2 eV in going from  $O_h$  to  $D_{3h}$  symmetry because it interacts less with the X lone pairs. The reason for the diminished interaction between  $z^2$  and the X lone pairs is shown in 2. The symmetry-



adapted linear combination of the X p orbitals to interact with  $z^2$  is symmetrical with respect to the  $xy$  plane and due to the shorter distances between eclipsed ligands in  $D_{3h}$  symmetry **2b** ( $D_{3h}$ ) is 0.8 eV lower in energy than **2a** ( $O_h$ ). As a consequence,  $z^2$  receives 0.26 electron from **2a** and only 0.17 from **2b** in  $D_{3h}$ .

The same phenomenon occurs for the two other orbitals,  $x^2 - y^2$  and  $xy$ , but the destabilization associated with the participation in the  $\sigma$  M–X bonds dominates and the two orbitals are higher in  $D_{3h}$  symmetry. Nonetheless, the overall diminished  $d_{\pi}/p_{\pi}$  interaction in  $D_{3h}$  geometry is apparent from the variation of the three lower d orbitals on going from  $O_h$  to  $D_{3h}$  geometry. For  $\text{WH}_6$ , they are destabilized by 1.5 eV. This value is divided by a factor 2–3 in the case of  $\text{WX}_6$  ( $X = \text{Cl, OH}$ ).

It is worth mentioning that a reverse effect was suggested by Hoffmann for a higher electron count.<sup>1</sup> For a  $d^6$  complex,  $\pi$ -acceptor ligands facilitate the  $O_h \rightarrow D_{3h}$  transformation by stabilizing the high-energy  $e'$  orbitals in  $D_{3h}$  symmetry. This suggestion was experimentally confirmed recently.<sup>21</sup> This illustrates the interplay between electron count and ligand  $\sigma$  and  $\pi$  effects.

It can thus be seen that there are several reasons for the preference for  $O_h$  symmetry in the case of  $\pi$ -donor groups. The  $t_{2g}$  orbitals responsible for the second-order J–T effect are higher with a  $\pi$  donor X, and therefore the participation of these orbitals in the M–X  $\sigma$  bonds in  $D_{3h}$  symmetry will be small. The  $d_{\pi}/p_{\pi}$  effects are less in trigonal prismatic geometry. Though the bielectronic repulsion between lone pairs on X is greater in trigonal prismatic geometry (relative to  $O_h$ ), this repulsion should be of little importance in the case of the tris(pinacolate) complex since the  $\sigma$  lone pairs are not pointing toward one another. It is therefore not surprising that, in the case of the tris(pinacolate) complex, where the alkoxy groups are excellent  $\pi$ -donor groups, the passage through  $D_{3h}$  geometry is significantly disfavored. A similar explanation has been given for distorted  $[\text{M}(\text{ndt})_3]^-$  ( $M = \text{Nb, Ta}$ ;  $\text{ndt} = \text{norbornane-exo-2,3-dithiolate}$ ) ( $\theta = 38.7^\circ$ ).<sup>22a</sup> Rigidity of the isomeric unit does not necessarily require bulky ligands.<sup>22b</sup>

(21) Karpishin, T. B.; Stack, T. D. P.; Raymond, K. N. *J. Am. Chem. Soc.* **1993**, *115*, 182.

(22) (a) Tatsumi, K.; Matsubana, I.; Inoue, Y.; Nakamura, A.; Miki, K.; Kasai, N. *J. Am. Chem. Soc.* **1989**, *111*, 7766. (b) Dietz, S. D.; Eilerts, N. W.; Heppert, J. A.; Morton, M. D. *Inorg. Chem.* **1993**, *32*, 1698.

(20) Avdeef, A.; Fackler, J. P., Jr. *Inorg. Chem.* **1945**, *14*, 2002.

## Experimental Section

All solvents were dried over Na(benzophenone) and distilled before use, and all reactions were performed under N<sub>2</sub> atmospheres using standard Schlenk and vacuum-line techniques. Proton NMR spectra were obtained in C<sub>6</sub>D<sub>6</sub> or C<sub>6</sub>D<sub>5</sub>CD<sub>3</sub> on a Variun 300 spectrometer operating at 299.66 MHz and referenced to residual solvent protio impurities at  $\delta = 7.15$  and 2.18 ppm, respectively. Variable-temperature <sup>1</sup>H NMR spectra were obtained from -90 to +110 °C and calibrated to an external methanol curve. Infrared spectra were obtained on samples as pressed KBr pellets on a Perkin-Elmer 283 spectrometer. Mass spectral data were obtained on a Kratos MS50. Microanalyses were provided by Oneida Research Services, Whiteboro, NY. Tungsten hexakis(dimethylamide) was prepared as previously described,<sup>23</sup> and pinacol was purchased from Aldrich Chemical Co. and used as supplied.

**W(O<sub>2</sub>C<sub>2</sub>Me<sub>4</sub>)<sub>3</sub> (1).** To W(NMe<sub>2</sub>)<sub>6</sub> (0.100 g, 0.22 mmol) in hexane/diethyl ether (15 mL/ 5 mL) at room temperature was added pinacol (0.67 mmol, 0.84 g) in diethyl ether (5 mL); this caused an immediate darkening of the solution to an orange-red. The mixture was allowed to stand at room temperature for 6 h, and then the solvent was removed *in vacuo*, leaving a brown solid. The solid was dissolved in the minimum volume of hot hexane (3 mL), the mixture was filtered through a Celite/glass frit, and the filtrate was cooled to -15 °C to produce large colorless crystals of W(O<sub>2</sub>C<sub>2</sub>Me<sub>4</sub>)<sub>3</sub> (0.158 mmol, 0.086 g, 72%). Microanal. Found: C, 40.81; H, 6.76. Calc: C, 40.60; H, 6.76. Mp = 182 °C (dec).

<sup>1</sup>H NMR in C<sub>6</sub>D<sub>6</sub> (25 °C):  $\delta = 1.54$  (s, 18H), 1.12 (s, 18H).

IR (cm<sup>-1</sup>): 2980 s, 2940 m, 2920 m, 2860 w, 1435 m, 1380 m, 1360 m, 1270 m, 1260 w, 1230 w, 1200 m, 1160 m, 1140 vs, 1100 w, 1090 w, 1070 w, 1020 w, 1000 m, 958 vs, 920 w, 885 vs, 850 w, 800 m, 700 vs, 620 vs, 555 w, 500 w, 450 w, 390 m, 325 m.

M/S (EI mode): M<sup>+</sup> (*m/z* 534), M<sup>+</sup> - C(CH<sub>3</sub>)<sub>2</sub>H, M<sup>+</sup> - OC(CH<sub>3</sub>)<sub>2</sub>H, M<sup>+</sup> - C<sub>2</sub>Me<sub>4</sub>O<sub>2</sub>, with the correct tungsten isotopic abundances.

**Crystallographic Determinations.** General operating procedures and a listing of programs have been given previously.<sup>24</sup> A summary of crystal data is given in Table 2. Atomic coordinates are given in Table 3.

A crystal of suitable size was cleaved from a large piece of the sample in a nitrogen-atmosphere glovebag. The crystal was mounted using silicone grease and was transferred to a goniostat where it was cooled to -155 °C for characterization and data collection. A systematic search of a limited hemisphere of reciprocal space revealed a C-centered cell with 2/*m* Laue symmetry. Following complete intensity data collection, the additional condition  $1 - 2n$  for *h*01 was observed. The choice of space group C2/*c* was later proven correct by the successful solution of the structure. After correction for absorption, data processing gave a residual of 0.022 for the averaging of complete 2-fold redundant data. Four standards measured every 300 data showed no significant trends.

**Table 3.** Fractional Coordinates and Isotropic Thermal Parameters (Å<sup>2</sup>) for W(O<sub>2</sub>C<sub>2</sub>Me<sub>4</sub>)<sub>3</sub> (1)

atom	10 <sup>4</sup> x	10 <sup>4</sup> y	10 <sup>4</sup> z	10B <sub>iso</sub>
W(1)	10 000	1138.2(2)	2500	9
O(2)	10 540(2)	802(3)	3984(2)	13
C(3)	11 164(3)	-251(5)	4341(4)	15
C(4)	11 607(3)	-215(5)	3474(3)	15
O(5)	10 915(2)	-14(3)	2501(2)	13
C(6)	11 742(3)	97(5)	5450(4)	18
C(7)	10 703(3)	-1578(5)	4347(4)	20
C(8)	12 211(3)	977(5)	3623(4)	18
C(9)	12 052(3)	-1527(5)	3385(4)	19
O(10)	10 560(2)	2647(3)	2122(2)	13
C(11)	10 188(3)	3974(4)	2039(4)	14
C(12)	9 514(3)	4104(5)	946(4)	19
C(13)	10 877(3)	5017(5)	2168(4)	22

The structure was solved using a combination of direct methods (MULTAN78) and Fourier techniques. The tungsten atom was located in an initial *E* map. The remaining non-hydrogen locations were obtained from subsequent iterations of least-squares refinement and difference Fourier calculations. Hydrogen atoms were included in fixed calculated positions. Hydrogen thermal parameters were fixed at 1 plus the isotropic thermal parameter of the atom to which they were bonded.

In the final cycles of refinement, the non-hydrogen atoms were varied with anisotropic thermal parameters to a final *R*(*F*) = 0.020. The final difference map was essentially featureless. There were tungsten residual peaks of 0.4–1.9 e/Å<sup>3</sup>. All other residual peaks were less than 0.4 e/Å<sup>3</sup>.

## Computational Procedures

The calculations were done with the extended Hückel method using the weighted *H*<sub>*ij*</sub> formula.<sup>25</sup> The atomic parameters were taken from the literature (W,<sup>26</sup> Cl<sup>27</sup>): W–H = 1.6 Å; W–Cl = 2.3 Å; W–O = 1.916 Å.

**Acknowledgment.** We thank the National Science Foundation for support and the NSF/CNRS for US/France international collaboration. I.P.P. acknowledges NATO for a postdoctoral fellowship.

**Supplementary Material Available:** Tables of crystallographic data, anisotropic thermal parameters, and complete bond distances and angles (4 pages). Ordering information is given on any current masthead page.

- (23) Bradley, D. C.; Chisholm, M. H.; Extine, M. W. *Inorg. Chem.* **1977**, *16*, 1791.  
 (24) Chisholm, M. H.; Folting, K.; Huffman, J. C.; Kirkpatrick, C. C. *Inorg. Chem.* **1983**, *24*, 1021.

- (25) Ammeter, J. H.; Bürgi, H.-B.; Thibault, J. C.; Hoffmann, R. *J. Am. Chem. Soc.* **1978**, *100*, 3686.  
 (26) Dedieu, A.; Albright, T. A.; Hoffmann, R. *J. Am. Chem. Soc.* **1979**, *101*, 3141.  
 (27) Summerville, R. H.; Hoffmann, R. *J. Am. Chem. Soc.* **1976**, *98*, 7240.